Free-Flight Dynamics of an Aeroshell/Drogue Parachute System

Juan R. Cruz[1]
NASA Langley Research Center, Hampton, Virginia, 23681-2199, United States of America

A free-flight test of a subscale aeroshell/drogue parachute model was conducted at the NASA Langley Research Center Vertical Spin Tunnel. Mass properties for the aeroshell model were dynamically scaled. This test simulated the flight of the Dragonfly mission spacecraft at an altitude of 18.4 km above the surface of Titan (Saturn's largest moon). The aeroshell/drogue parachute model exhibited bimodal oscillatory behavior with sustained small- and large-amplitude modes depending on initial conditions. The effects of drogue parachute size, bridle geometry, and bridle rigidity on the aeroshell/drogue parachute dynamics were investigated. The large-amplitude oscillations seemed to be driven by the aeroshell aerodynamics, with bridle leg collapse being an enabling factor. If the bridle legs were rigid, large-amplitude oscillations were not sustainable.

Nomenclature

C_D	=	drogue parachute drag coefficient without aeroshell (model); based on S_0 as the reference area
C_DS_0	=	drogue parachute drag area without aeroshell (model)
D_A	=	aeroshell diameter (model)
D_0	=	drogue parachute nominal diameter (model)
$D_{0,FS}$	=	drogue parachute nominal diameter (full-scale)
m_A	=	aeroshell mass (model)
I_{xx}, I_{yy}, I_{zz}	=	mass moments of inertia of the aeroshell about its center of mass and x-, y-, z- axes, respectively (model)
S_0	=	drogue parachute nominal area (model)
X_{VST}, Y_{VST}, Z_{VST}	=	Cartesian coordinate system fixed to the VST; used to determine the position of the aeroshell model within the VST
x, y, z	=	aeroshell axes; the x-axis is coincident with the axis of symmetry of the aeroshell, pointing upstream; the y- and z-axes complete the Cartesian coordinate system; the origin of the axes are at the center of mass of the aeroshell (model)
x_{CoM}	=	aeroshell center of mass position downstream of the nose along the x-axis (model)
γ	=	angle used to illustrate bridle leg collapse
Θ	=	nadir angle; angle between the aeroshell axis of symmetry and the local vertical
LaRC	=	Langley Research Center
VST	=	Vertical Spin Tunnel

I. Introduction

A free-flight test of the Dragonfly mission aeroshell/drogue parachute system was performed to investigate its dynamic behavior. (Subsequently in this paper "drogue parachute" will be simply referred to as "parachute.") The test was conducted using a subscale aeroshell model whose mass properties was dynamically scaled. (All subsequent

[1] Aerospace Engineer, Atmospheric Flight and Entry Systems Branch, AIAA Associate Fellow.

references to the aeroshell and parachute are to the model unless otherwise stated.) A variety of design variations were tested including changing the parachute size and bridle attachment between the aeroshell and parachute. The test took place at the NASA Langley Research Center (LaRC) Vertical Spin Tunnel (VST) at low subsonic speeds. This paper describes the test and its results.

II. Wind Tunnel Model

A. Aeroshell

A photo of the aeroshell is presented in Figure 1, and a drawing is shown in Figure 2. The geometry of the aeroshell is a scaled version of that used for the Genesis mission. (Ref. 1). The aeroshell was fabricated at a scale of 6.67%, yielding a diameter, D_A, of 0.300 m (full-scale 4.5 m). The dynamically-scaled mass properties of the aeroshell were as shown in Table 1. With these mass properties the aeroshell simulated flight on Titan at an altitude of 18.8 km. In full-scale at this altitude the aeroshell is descending at a Mach number of approximately 0.05. Thus, compressibility effects are negligible.

Figure 1. Aeroshell, bridle, and parachute. (NASA LaRC photo)

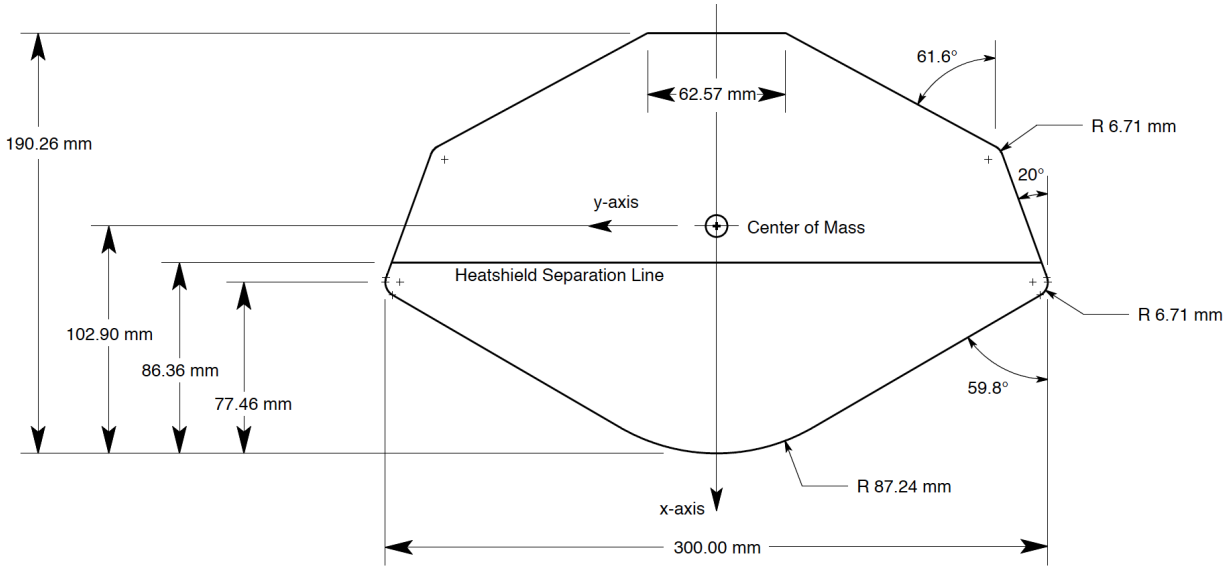

Figure 2. Aeroshell drawing.

Table 1. Aeroshell mass properties.

Property	Value
m_A, Mass	249 g
Center of mass, x_{CoM}	0.1035 m downstream of nose, on the axis of symmetry of the aeroshell
Mass moment of inertia about the x-axis, I_{xx}	2161 kg•mm^2 (the x-axis is coincident with the axis of symmetry of the aeroshell)
Mass moment of inertia about the y-axis, I_{yy}	1343 kg•mm^2
Mass moment of inertia about the z-axis, I_{zz}	1614 kg•mm^2

B. Bridles

The attachment of the parachute to the aeroshell affects the dynamic behavior of the system. The parachute is attached to the rear surface of the aeroshell through a bridle (seen as white cords on top of the aeroshell in Figure 1). The bridles used for this test had either one, three, or four legs. The geometry of the bridles used during the test (side and top views including bridle height and attachment points) are shown in Figure 3a and 3b. Because the bridles were made of cords, each leg of the bridle was a tension-only element (except in the instances described below). As shown in Figure 4, if the force of the parachute is applied at a sufficiently large angle off the axis of symmetry of the aeroshell, one or more legs of the bridle will collapse (exceptions to this statement occurs when: 1) there is only a single bridle leg or, 2) the legs of the triple bridle are not cords but instead are rigid – in this case none of the legs will collapse regardless of the force direction). The angles at which the legs will collapse depend on the bridle geometry and the clock angle at which the force is being applied. Table 2 shows the minimum and maximum collapse angles for the bridles used in the test. The physical consequence of a leg collapse is that the restoring moment provided by the parachute is diminished (as compared to that of a rigid bridle) since the moment arm (i.e., the distance from the aeroshell center of mass to the point at which the parachute force acts on the aeroshell) is smaller when a bridle leg has collapsed.

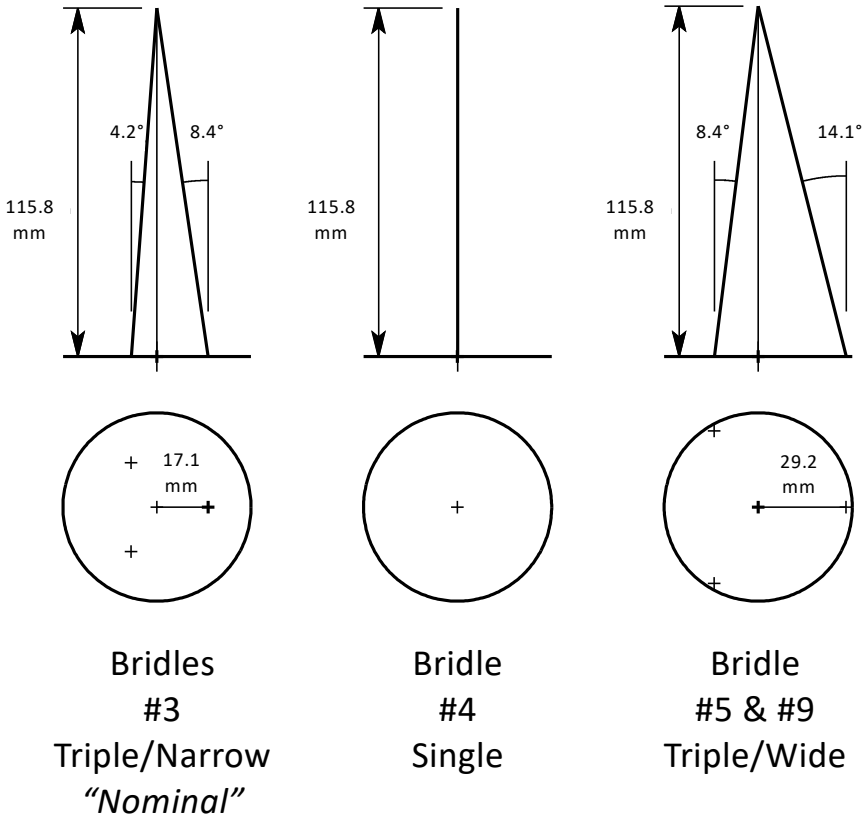

Figure 3a. Geometries for bridles #3, #4, #5, and #9; side and top views.

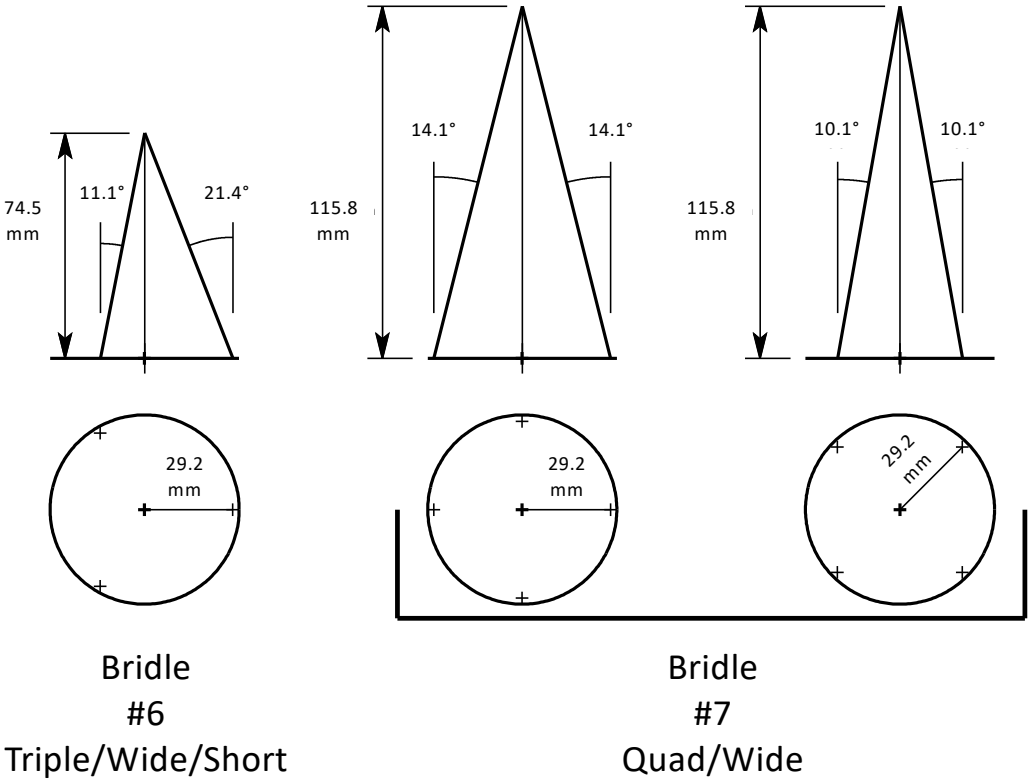

Figure 3a. Geometries for bridles #6 and #7; side and top views.

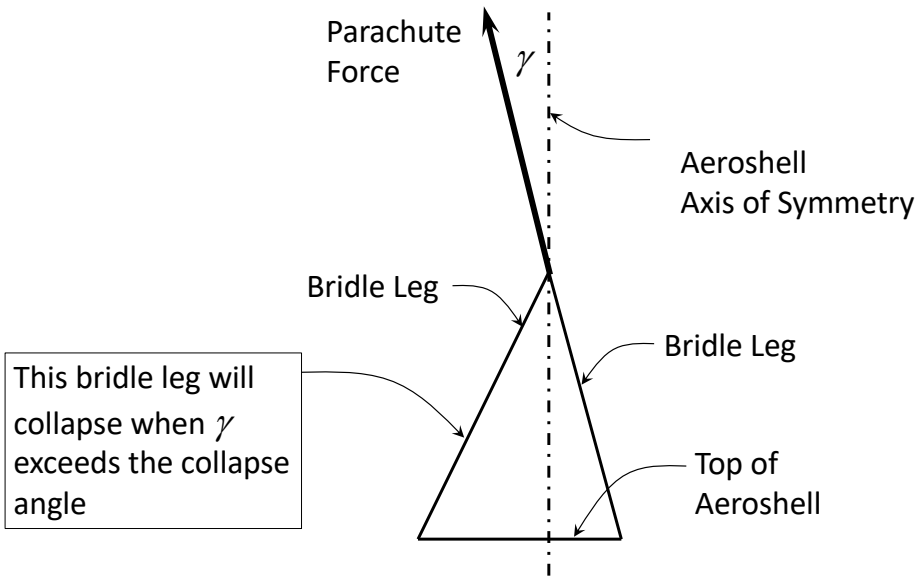

Figure 4. Parachute force and bridle leg collapse.

Table 2. Bridle legs collapse angles.

Bridle	Name	Min Collapse Angle	Max Collapse Angle
#3	Triple/Narrow (Nominal)	4.2°	8.4°
#4	Single	Not Applicable	Not Applicable
#5	Triple/Wide	7.2°	14.1°
#6	Triple/Wide/Short	11.1°	21.4°
#7	Quad/Wide	10.1°	14.1°
#9	Triple/Wide/Rigid	Not Applicable	Not Applicable

Notes:

1) Bridle ID #3, Triple/Narrow, is considered to be the "Nominal" bridle geometry.
2) The Single (Bridle ID #4) and Triple/Wide/Rigid (Bridle ID #9) bridles do not have collapse angles associated with them.
3) Bridle #9, Triple/Wide/Rigid was rigidized by fabricating the legs from piano wire; this prevented the legs from collapsing.

C. Parachutes

The parachutes used were selected from the available stock at the VST. These parachutes are flat circular canopies without a vent and a suspension line-to-diameter ratio of approximately 1. They are fabricated from a gauze-like material. The mass properties of the parachutes were not dynamically scaled. Based on free-flight measurements at the VST using ballast weights, the parachutes drag coefficient, C_D, without the aeroshell was estimated to be 0.65 using their nominal area, S_0, as the reference area. Three parachute sizes were used as shown in Table 3: small, nominal, and large. Their equivalent full-scale parachute diameters are shown in the last two columns of Table 3. The scaling based on parachute diameter is simply a geometric calculation. The scaling based on drag area assumes that the full-scale parachute has a nominal diameter of 5.4 m, and a drag coefficient based on its nominal area of 0.58.

Table 3. Parachutes

Parachute	Nominal Diameter, D_0 (m)	Nominal Area, S_0 (m^2)	Drag Area, C_DS_0 (m^2)	Drag Area Ratio (wrt. Nominal)	Full-Scale Nominal Diameter Based on Diameter, $D_{0,FS}$ (m)	Full-Scale Nominal Diameter Based on Drag Area, $D_{0,FS}$ (m)
Small	0.255	0.0510	0.0331	0.45	3.83	4.05
Nominal	0.381	0.1137	0.0739	1.00	5.72	6.04
Large	0.409	0.1314	0.0854	1.16	6.14	6.49

The parachute is attached to the bridle through a long riser. The length of this riser is determined by considerations that are mainly important at supersonic speeds (i.e., during and immediately after parachute deployment in the full-scale system). For the present test the riser length was set so that the trailing ratio, (distance from the aeroshell maximum diameter to the parachute skirt) / (aeroshell diameter), was 10 when using nominal parachute and bridle. This resulted in a riser length of slightly less than 3.0 m. The value of this trailing ratio varied slightly during the test due to changes in the bridle geometry and the different suspension line lengths for the small and large parachutes.

The dynamic motions of the parachute by themselves (i.e., while tested with the ballast weights) were observed to be very "stable" in the sense that their trim total angle of attack was small, and oscillations were of small amplitude. (This observation will be relevant during the following discussion of the aeroshell/parachute dynamics.)

III. Test Facility

The test was conducted at the NASA LaRC Vertical Spin Tunnel (VST). This facility is a vertical-flow tunnel that allows the free-flight of models. A cross-section of the VST is shown in Figure 5. The VST is 6.1 m (20 ft) across and about 7.6 m (25 ft) tall from net-to-net. The model is kept "flying" within the bounds of the nets by adjusting the airspeed in the VST by changing the speed of the electric motor driving the fan at the top of the test section. Motor speed is controlled in real time by an operator observing the model.

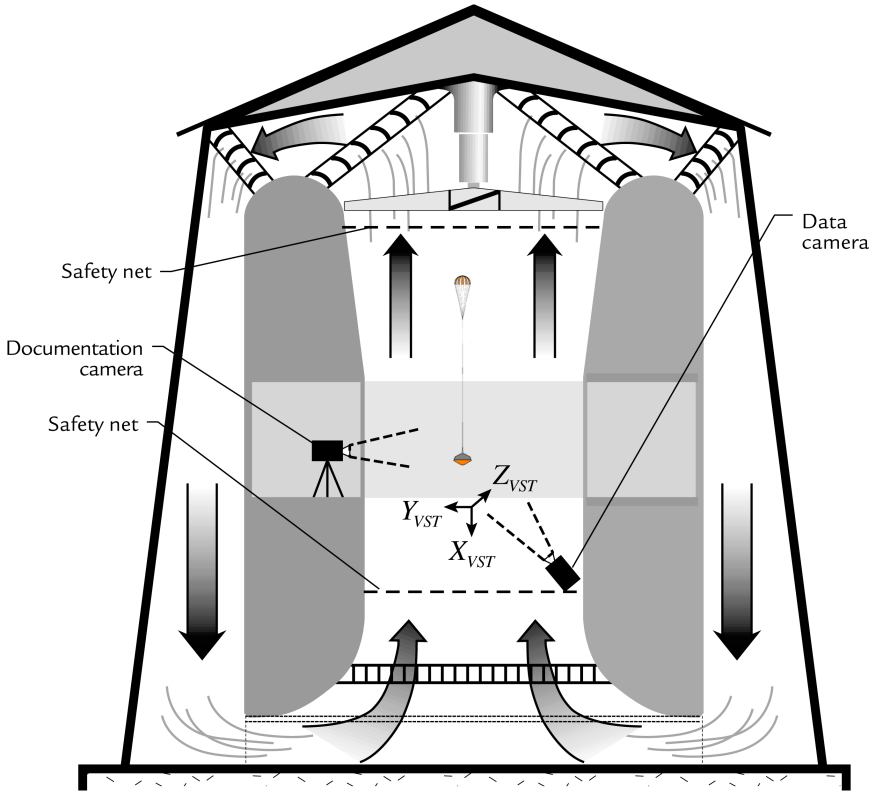

Figure 5. Vertical Spin Tunnel cross section view. (NASA LaRC image)

Instrumentation in the VST allows for the determination and recording of dynamic pressure, static pressure, temperature, airspeed, position of the aeroshell, and attitude of the aeroshell versus time. The position and attitude of the aeroshell are obtained by a motion capture system which observes the position of reflective dots placed on the aeroshell. The output of this motion capture system is the position of the aeroshell in the VST-fixed coordinate system (X_{VST}, Y_{VST}, Z_{VST}), and a set of Euler angles. Various options are available for the selection of coordinate system orientation and Euler angles definitions. In addition, a video documentation camera is used to record the motions of the aeroshell and provide a qualitative record of the test.

IV. Test Procedure and Data Collection

The test procedure was as follows:

1) The VST airspeed was brought up to an appropriate value for the specific aeroshell/parachute configuration.
2) Data collection was initiated.
3) A technician placed the aeroshell/parachute in the airstream through an open window in the VST and released it; see Figure 6. Two release methods were used: unperturbed launch and perturbed launch. With an unperturbed launch the aeroshell was released upright with minimal pitch/yaw angles and rates. With a perturbed launch the aeroshell was released inverted with large pitch/yaw rates. For all launches no intentional roll rate (i.e., rotation rate about the *x*-axis) was intentionally induced.
4) The VST operator adjusted the throttle to maintain the aeroshell/parachute within the bounds of the upper and lower safety nets (see Figure 5).
5) A particular test run was concluded when the aeroshell/parachute touched any portion of the VST (e.g., safety nets, walls).
6) At the end of a run data collection was stopped, and the aeroshell/parachute retrieved for another run.

Figure 6. Aeroshell/parachute release in the VST. The technician is holding the aeroshell. This particular photograph shows an unperturbed launch. Note the length of the riser and the parachute at its end. (NASA LaRC photo)

The data collected was dynamic pressure, static pressure, temperature, airspeed, position of the aeroshell, and attitude of the aeroshell, at a rate of 150 Hz. A minimum of approximately 10 seconds was required for a given test run to be considered successful. Maximum test run lengths were about 60 seconds. Video was recorded of the aeroshell through one of the test section windows for qualitative analyses.

V. Data Analyses

Extensive analyses of the data were conducted. In this paper only one parameter is discussed – the nadir angle, Θ, its time histories and statistics. The nadir angle is the angle between the aeroshell's axis of symmetry and the vertical as shown in Figure 7. The nadir angle was calculated using two of the Euler angles obtained from the motion capture system. This angle captures the essence of the aeroshell dynamics of interest.

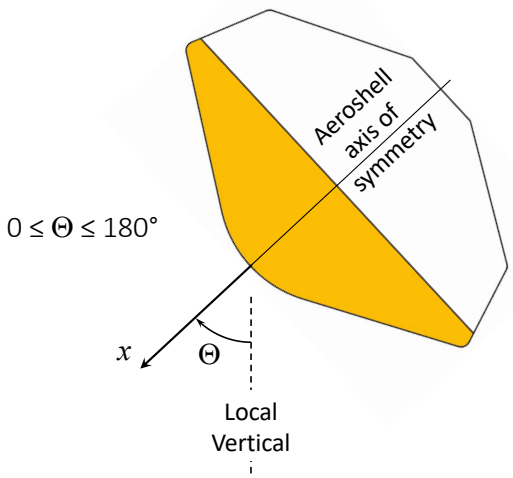

Figure 7. Definition of the nadir angle, Θ.

Once a time history of Θ versus time was obtained, the peaks and 90 percentile values of the Θ peaks were calculated. This process is illustrated in Figure 8. From the time history of Θ versus time (Step 1) the peaks in the oscillations were identified (Step 2). The cumulative probability of peak Θ values were obtained (Step 3), with particular interest in the 90 percentile value. Data from all available runs with the same parachute/bridle configuration (i.e., "Block" as defined below) and oscillatory behavior (i.e., small- or large-amplitude oscillations as described below) were combined to determine the cumulative probability. The 90 percentile value of the peak Θ cumulative probability was considered to be a good metric of the aeroshell dynamics.

Step 1: Obtain Θ vs. time

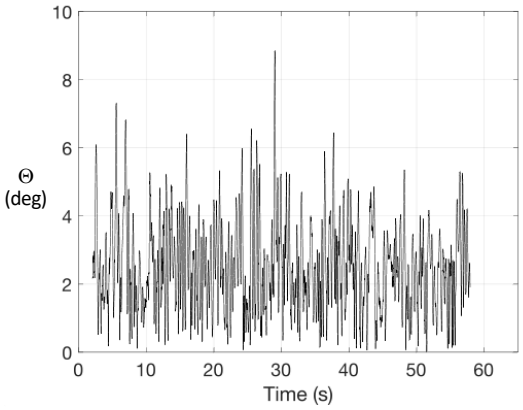

Step 2: Identify Θ peaks

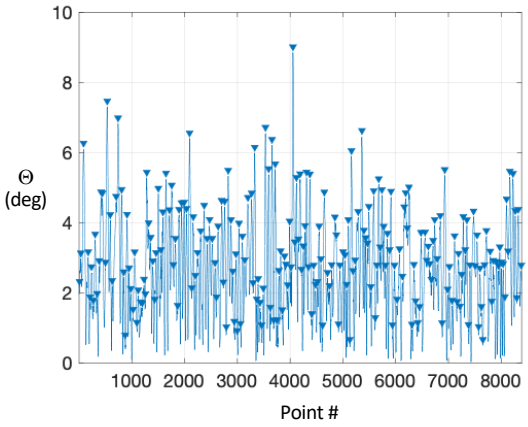

Step 3: Calculate peak Θ cumulative probability

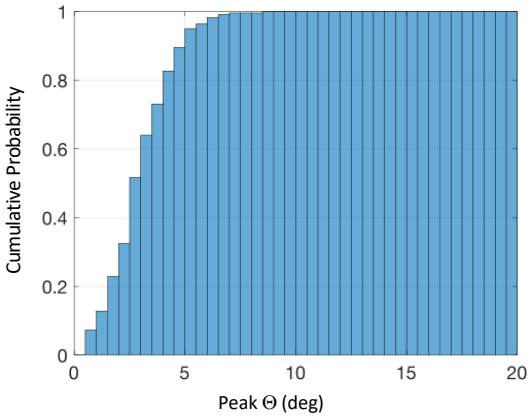

Figure 8. Identification of the statistics for peak Θ.

VI. Results

The test was conducted in Blocks. Each Block had a specific parachute/bridle configuration. The configurations of these Blocks are shown in Table 4. Block 9 was considered to be the Baseline configuration. Within a Block, there are a number of individual tests denoted as runs. For all Blocks, runs were conducted using both unperturbed and perturbed launches.

Table 4. Test matrix.

Block	Parachute	Bridle
9	Nominal	#3, Triple/Narrow (Nominal)
10	Large	#3, Triple/Narrow (Nominal)
11	Small	#3, Triple/Narrow (Nominal)
12	Nominal	#4, Single
13	Nominal	#5, Triple/Wide
14	Nominal	#6, Triple/Wide/Short
15	Nominal	#7 Quad/Wide
16	Nominal	#9 Triple/Wide/Rigid

A sample set of time histories for the Baseline configuration (Block 9) are shown in Figure 9. This figure shows that the aeroshell had two distinct (i.e., bimodal) dynamic modes: a small Θ oscillation and a large Θ oscillation. The persistence of the oscillations indicate that these two modes are "stable" meaning that they will continue indefinitely in the absence of external influences.

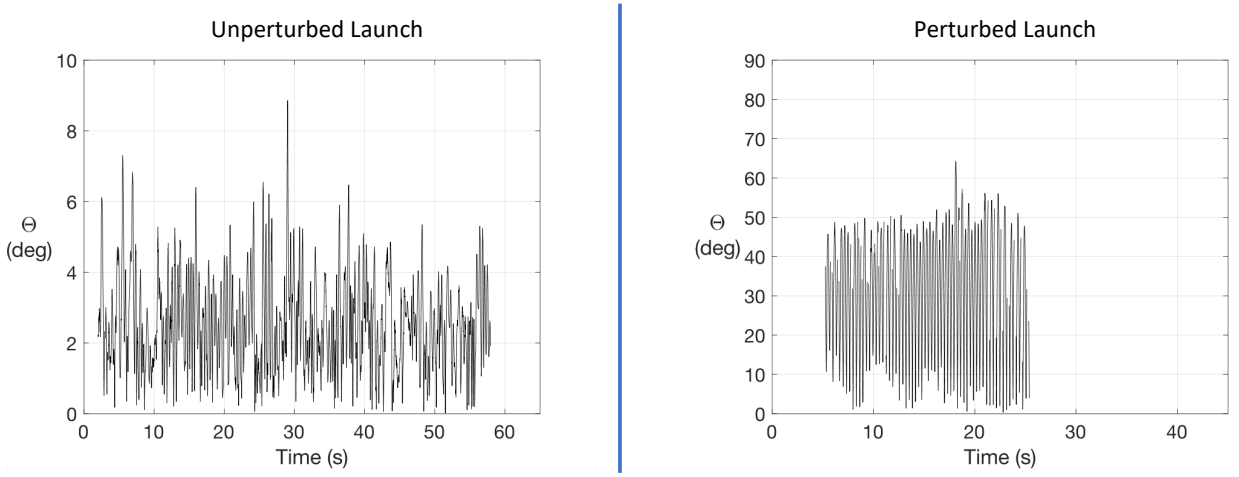

Figure 9. Dynamic behavior of the Baseline configuration (Block 9, Nominal parachute, Bridle #3 Triple/Narrow) with unperturbed and perturbed launches.

A summary of the results are shown in Table 5. Based on these results the following observations can be made.

1) Bimodal oscillatory behavior (i.e., the presence of both small and large Θ oscillations) was observed for all aeroshell/parachute configurations except for Block 17 (Nominal parachute, Bridle #9 Triple/Wide/Rigid) which incorporated a rigid bridle. (Further observations related to the results of Block 17 are included below.)
2) For all aeroshell/parachute configurations the small Θ oscillatory behavior had a 90 percentile peak of 5.35° ± 0.55°. Differences in parachute size and bridle geometry had a small influence (± 0.55°) on the amplitude of the small Θ oscillatory behavior.
3) For all aeroshell/parachute configurations exhibiting bimodal behavior (Blocks 9-15) the large Θ oscillatory behavior had a 90 percentile peak of 53.8° ± 5.8° except for Block 11 which used a small parachute. Differences in bridle geometry for the nominal and large parachute sizes in Blocks 9, 10,

and 12-15 made only a relatively small (± 5.8°) difference in the large Θ oscillatory behavior. When using a small parachute (Block 11) the large Θ oscillations had a 90 percentile peak of 82.3°, this value was significantly larger than the average value for the other configurations exhibiting bimodal behavior (53.8°).

4) When using a rigid bridle (Block 17) the aeroshell could not be made to exhibit bimodal oscillatory behavior. Out of 29 perturbed launches none yielded large Θ oscillatory behavior; only the small Θ oscillatory behavior was observed. This aeroshell/parachute configuration points out the importance of bridle leg collapse in the large Θ oscillatory behavior.
5) The configurations using wide non-rigid bridles (i.e., Blocks 13, 14, and 15), exhibited large Θ oscillatory behavior, however, it was more difficult to cause this behavior. Note (from Table 5) that the number of launches that yielded large Θ oscillations was less than 100%. Note that for the Block 13, 14, and 15 configurations the bridle legs collapse angles are larger (see Table 2). This observation brings out the importance of bridle leg collapse in the large Θ oscillatory behavior.
6) Given the previous observation regarding the parachutes stability (i.e., that the parachutes are stable by themselves, see Section II.C), it seems that the large Θ oscillation are principally due to the aerodynamics aeroshell, not the parachutes. The results obtained with the rigid triple bridle (Block 17) indicate that bridle leg collapse enable large Θ oscillations but is not the cause.

Table 5. Summary of test results.

Block	Parachute	Bridle	90%-tile Small Θ (deg)	90%-tile Large Θ (deg)	Comments
9	Nominal	#3, Triple/Narrow (Nominal)	5.0	53.5	Baseline configuration. 100% of perturbed launches yielded sustained large Θ oscillations (14/14).
10	Large	#3, Triple/Narrow (Nominal)	5.4	53.2	100% of perturbed launches yielded sustained large Θ oscillations (9/9).
11	Small	#3, Triple/Narrow (Nominal)	5.9	82.3	100% of perturbed launches yielded sustained large Θ oscillations (6/6).
12	Nominal	#4, Single	5.3	59.6	100% of perturbed launches yielded sustained large Θ oscillations (8/8).
13	Nominal	#5, Triple/Wide	5.2	49.5	18% of perturbed launches yielded sustained large Θ oscillations (2/11).
14	Nominal	#6, Triple/Wide/Short	4.8	52.8	75% of perturbed launches yielded sustained large Θ oscillations (6/8).
15	Nominal	#7, Quad/Wide	4.9	48.0	31% of perturbed launches yielded sustained large Θ oscillations (4/13).
17	Nominal	#9, Triple/Wide/Rigid	5.3	None	0% of perturbed launches yielded sustained large Θ oscillations (0/29).

VII. Concluding Remarks

The free-flight test described in this paper met its goal of providing information on the Dragonfly aeroshell/parachute system at subsonic speeds. Key observations resulting from the test are:

a) For most aeroshell/bridle/parachute configurations the aeroshell exhibits a bimodal oscillatory behavior that leads to either small- or large-amplitude modes. Which mode is excited depended on the aeroshell launch conditions (i.e., unperturbed or perturbed). A sufficiently violent initial condition is required for the large-amplitude oscillation mode to occur.
b) The large-amplitude oscillation mode seems to be driven by the aeroshell aerodynamics.
c) Bridle leg collapse is an enabling factor for the large-amplitude oscillation mode. If the bridle is rigid, sustained large-amplitude oscillations are not possible.

d) Wider bridle attachment footprints makes it more difficult for the large-amplitude oscillation mode to occur.
e) The aeroshell/parachute configuration with the small parachute has a large-amplitude oscillation mode of significantly higher magnitude than those for the nominal and large parachutes.

An important point to consider in evaluating the results presented herein is the operating Reynolds number mismatch between the model and full-scale systems. Although the model aeroshell has appropriate geometric and mass properties scaling, the operating Reynolds number of the model is a small fraction of that in full-scale flight. Given the differences in the atmosphere and acceleration of gravity between Titan and Earth this difference in operating Reynolds number is inevitable. Future tests are planned to understand and minimize the effects of Reynolds number on the dynamics of the aeroshell/parachute system.

Acknowledgments

The model aeroshell was fabricated by staff at NASA LaRC. Testing at the VST was conducted with by Bruce D. Owens and Clinton Duncan of the NASA LaRC Flight Dynamics Branch. The help of all these individuals is gratefully acknowledged.

References

[1] Desai, P. N. and Cheatwood, F. McNeil, "Entry Dispersion Analysis for the Genesis Sample Return Capsule," Journal of Spacecraft and Rockets, Vol. 38, No. 3, May-June 2001, pp. 345-350.